12

Simulating the Response of Structures to Impulse Loadings

Soprano Alessandro and Caputo Francesco
Second University of Naples
Italy

1. Introduction

The need to cope with the new problems which are coupled with progress and its challenges has been causing new design and analysis methodologies to appear and develop; thus, beside the original concept of a structure subjected to statically applied loads, new criteria have been devised and new scenarios analyzed. From fatigue to fracture, vibrations, acoustic, thermomechanics, to remember just a few, many new aspects have been studied in course of the years, all taking place in connection with the appearance of new technical or technological problems, or even with the growing of the consciousness of the relevance of such aspects as safety, reliability, maintenance, manufacturing costs and so on.
One of the problems which in the recent years has been increasingly considered as a relevant one is that of the behaviour of structures in the case of impact loading; there are many reasons for such a study: for example, the requirement to ensure a never-too-satisfactory degree of safety for the occupants of cars, trains or even aircrafts in impact conditions, preventing any collision with the interiors of the vehicle, is just one case.
Another case to be mentioned is that connected with mechanical manufacturing or assembling, which is often carried out with such an high speed as to induce impulse loadings into the involved members; in such cases the aim is to obtain a sound result, even a 'robust' one, in the sense that the same result is to be made as independent as possible from the conceivable variations of the input variables, which, in turn, can be only defined on a probabilistic basis, due for example to their manufacturing scatter and tolerances.
Two main aspects arise in such problems, the first being that related to the definition of the mechanical properties of the materials; the analysis of members behaviour under impulsive loading, for example, requires in general the knowledge of the characteristic curves of materials in presence of high strain rates, which is not usually included in the standard tests which are carried out, so that new experimental tests have to be devised in order to obtain the required items. But at the same time new material families are generated daily, for which no test history is available; in the case of plastics and foams, for example, the search for a reliable database is often a very hard task, so that the analyst has to become a test driver, designing even the test which is the most efficient to obtain effectively the data he needs.
The second problem is the one related to the complication of the geometry and that is adding on the complexity of the analysis of the load conditions. In such cases it is just natural and obvious to direct the own attention to numerical methods, thanks to the ever-

increasing capabilities of computers and commercial codes, and, first of all, to Finite Element Methods (FEM).
FEM, as everything else, is no longer what it used to be in the '70s, when it could scarcely afford to deal with rather easy problems in presence of static conditions, at least from a practical point of view and apart from theory. Nowadays there are commercial codes which can deal with some millions of degrees of freedom (dof's) in static as well dynamic load conditions. The development of numerical procedures which, applying lagrangian and eulerian formulations for finite strains and stresses, allow the analysis of non-linear continua, the use of particular routines for time integration and the progress of the theory of constitutive law for new materials are just a few of the elements, which not only let today researchers investigate rare and particular behaviours of structures, but also allow the birth of rather easy-to-use codes which are increasingly adopted in industrial environments.
Even with such capabilities, the use of the classical "implicit finite element method" encounters many difficulties; therefore, one has to use other tools, and first of all the "explicit FEM", which is well fitted to study dynamic events which take place in very short time intervals. That doesn't mean that analysts don't find relevant difficulties when studying the behaviour of structures subjected to impulsive loads; for example, one has usually to use very short steps in time integration, which causes such analyses to be very time-consuming, even more as one has to overcome serious problems in the treatment of the interface elements used to simulate contact and to represent external loads; at last, only first-order elements (four-node quadrilaterals, eight-node bricks, etc.) are available in the present versions of the most popular commercial codes, what requires very fine meshes to model the largest part of members and that in turn asks for even shorter time steps.
In the following sections, after briefly recalling the main aspects of explicit FEM, we illustrate some of the problems encountered in the study of relevant cases pertaining to the fields of metalformig and manufacturing as well as crashworthiness and biomechanical behaviour, all coming from the direct experience of the authors.

2. Main aspects of explicit FEM

Finite element equations can be written according to Lagrangian or Eulerian formulations; in the former the material is fixed to the finite element mesh which deforms and moves with the material; in Eulerian space the finite element mesh is stationary and the "material flows" through this mesh, what is well suited for fluid dynamic problems. As most structural analysis problems are expressed in Lagrangian space, most commercial codes develop their finite element formulation in that space, even if all of them include algorithms based on Arbitrary Lagrangian-Eulerian (ALE) formulation to face fluid-like material simulation.
To solve a problem of a three-dimensional body located in a Lagrangian space, subjected to external body forces $b_i(t)$ (per unit volume) acting on its whole volume V, traction forces $t_i(t)$ (per unit area) on a portion of its outer surface S_t, and prescribed displacements $d_i(t)$ on the surface S_d, one must seek a solution to the equilibrium equation:

$$\sigma_{ij,j} + \rho b_i - \rho \ddot{x}_i = 0 \,, \tag{1}$$

satisfying the traction boundary conditions over the surface S_t:

$$\sigma_{ij} n_j = t_i(t) \,, \tag{2}$$

and the displacement boundary conditions over S_d:

$$x_i\left(X_a,t\right)=d_i\left(t\right), \tag{3}$$

where σ_{ij} is Cauchy's stress tensor, ρ is the material density, n_j is the outward normal unit vector to the traction surface S_t, X_α (α=1,2,3) and x are the initial and current particle coordinates and *t* is current time.

These equations state the problem in the so-called "strong form", which means that they are to be satisfied at every point in the body or on its surface; to solve a problem numerically by the finite element method, however, it is much more convenient to express equilibrium conditions in the "weak form" where the conditions have to be met only in an average or integral sense.

In the weak form equation, we introduce an arbitrary virtual displacement δx_i that satisfies the displacement boundary condition in S_d. Multiplying equilibrium equation (1) by the virtual displacement and integrating over the volume of the body yields:

$$\int_V\left(\sigma_{ij,j}+\rho b_i-\rho\ddot{x}_i\right)\delta x_i dV=0, \tag{4}$$

by operating simple substitutions and applying traction boundary condition, eq. (4) can be reworked as:

$$\int_V \rho\ddot{x}_i\delta x_i\,dV+\int_V \sigma_{ij}\delta x_{i,j}\,dV-\int_V \rho b_i\delta x_i\,dV-\int_{S_t} t_i\delta x_i\,dS=0 \tag{5}$$

which represents the statement of the principle of virtual work for a general three-dimensional problem.

The next step in deriving the finite element equations is spatial discretization. This is achieved by superimposing a mesh of finite elements interconnected at nodal points. Then shape functions (N_α) are introduced to establish a relationship between the displacements at inner points of the elements and those at the nodal points:

$$\delta x_i=\sum_{a=1}^{n}N_a\delta x_{ai} \tag{6}$$

This task governs all numerical formulations based on the finite element method, whose equations are obtained by discretizing the virtual work equation (5) and replacing the virtual displacement with eq. (6) between the displacements at inner points in the elements and the displacements at the nodal points:

$$\sum_{m=1}^{M}\left\{\int_{V_m}\rho N_a N_\beta\,dV_m\right\}\ddot{x}_{\beta i}=\sum_{m=1}^{M}\int_{V_m}N_a\rho b_i\,dV_m+\sum_{m=1}^{M}\int_{S_t}N_a t_i\,dS_m-\sum_{m=1}^{M}\int_{V_m}N_{a,j}\sigma_{ij}\,dV_m \tag{7}$$

where M is the total number of elements in the system and V_m is the volume of an element.

In matrix form, eq. (7) becomes:

$$\left[\mathbf{M}\right]\left\{\ddot{\mathbf{x}}\right\}=\left\{\mathbf{F}\right\} \tag{8}$$

where [**M**] is the mass matrix, $\ddot{\mathbf{x}}$ is the acceleration vector, and {**F**} is the vector summation of all the internal and external forces. This is the finite element equation that is to be solved at each time step.

The time interval between two successive instants, t_{n-1} and t_n , is the time step $\Delta t_n = t_n - t_{n-1}$; in numerical analysis, integration methods over time are classified according to the structure of the time difference equation. The difference formula is called explicit if the equation for the function at time step *n* only involves the derivatives at previous time steps; otherwise it is called implicit. Explicit integration methods generally lead to solution schemes which do not require the solution of a coupled system of equations, provided that the consistent mass matrix is superseded by a lumped mass one, which offers the great advantage to avoid solving any system equations when updating the nodal accelerations.

In computational mechanics and physics, the central difference method is a popular explicit method.

The explicit method, however, is only conditionally stable, i.e. for the solution to be stable, the time step has to be so small that information do not propagate across more than one element per time step. A typical time step for explicit solutions is in the order of 10^{-6} seconds, but it is not unusual to use even shorter steps. This restriction makes the explicit method inadequate for long dynamic problems. The advantages of the explicit method are that the time integration is easy to implement, the material non-linearity can be cheaply and accurately treated, and the computer resources required are small even for large problems. These advantages make the explicit method ideal for short-duration nonlinear dynamic problems, such as impact and penetration.

The time step of an explicit analysis is determined as the shortest stable time step in any deformable finite element in the mesh. The choice of the time step is a critical one, since a large time step can result in an unstable solution, while a small one can make the computation inefficient: therefore, an accurate estimation has to be carried out.

Generally, time steps change with the current time; this is necessary in most practical calculations since the stable one will change as the mesh deforms. This aspect can make the total runtime unpredictable, even if some "tuning algorithms" implemented in the most popular commercial codes try to avoid it; for example, as that change is required if high deformations are very localized in the model, one can add some masses to the nodes in the deformed area, but not so much to influence the global dynamic behaviour of the structure.

The same tuning process, which leads to added mass to the initial model in those areas where the element size is smaller, can be used to allow an initial time step which is longer than the auto-calculated one. As stated above, the critical time step has to be small enough such that the stress wave does not travel across more than one element at each time step.

This is achieved by using the Courant criteria:

$$\Delta t_e = l/c \tag{9}$$

where Δt_e is the auto-calculated critical time step of an element in the model, l is the characteristic length, and c is the wave speed. The wave speed, c, can be expressed as:

$$c = \sqrt{\frac{E}{\rho\left(1-\nu^2\right)}} \tag{10}$$

where E, ρ and ν are the Young's modulus, density and Poisson's ratio of the material respectively. Therefore, increasing ρ results in an artificial decrease of c and in a parallel increase of Δt_e, without varying the mechanical properties of the material.
The time step of the system is determined by taking the minimum value over all elements:

$$\Delta t_{n+1} = a \cdot \min\left\{\Delta t_1, \Delta t_2, \Delta t_3, \ldots, \Delta t_M\right\} \tag{11}$$

where M is the number of elements. For stability reasons, the scale factor α is typically set to a value of 0.9 (the default in the most popular commercial code, as for example in the LS-Dyna® code) or some smaller value.
Another aspect to be strongly considered when we deal with explicit finite element method is the contact definition, which allows to model the interactions between one or more parts in a numerical model and which is needed in any large deformation problem. The main objective of the contact interfaces is to eliminate any `overlap` or `penetration` between the interacting surfaces. Depending on the type of algorithm used to remove the penetration, both energy and momentum are preserved.
The contact algorithms can be mainly classified into two main branches, one using the penalty methods, which allow penetration to occur but penalize it by applying surface contact force models; the other uses the Lagrange multiplier methods which exactly preserve the non-inter-penetration constraint.
The penalty approach satisfies contact conditions by first detecting the amount of penetration and then applying a force to remove them approximately; the accuracy of approximate solutions depends strongly on the penalty parameter, which is a kind of "stiffness" by which contact surfaces react to the reciprocal penetration. This method is widely used in complex three-dimensional contact–impact problems since it is simple to use in a finite-element solving system. However, there are no clear rules to choose the penalty parameter, as it depends on the particular problem considered. On the other hand, the penalty method affects the stability of the explicit analysis, which is only conditionally stable, when the penalty parameter reaches a certain value with reference to the real stiffness of the material of the interacting surfaces.
Unlike the penalty method, the Lagrange multiplier method doesn't use any algorithmic parameters and it enforces the zero-penetration condition exactly. Thus, this method can give out very accurate displacement fields in the analysis of static contact problems; however, for dynamic contact problems it requires the solution of implicit augmented systems of equations, which can become computationally very expensive for large problems and therefore it is rarely used in solid mechanics field.
Effectively, a contact is defined by identifying what locations are to be checked for potential penetration of a slave node through a master segment. A search for penetrations, using the chosen algorithm, is made every time step. In the case of a penalty-based contact, when a penetration is found a force proportional to the penetration depth is applied to resist, and ultimately to eliminate, the penetration. Rigid bodies may be included in any penalty-based contact but if contact force are to be realistically distributed, it is recommended that the mesh defining any rigid body are as fine as those of any deformable body.
Though sometimes it is convenient and effective to define a single contact to handle any potential contact situation in a model, it is admissible to define a number whatever of contacts in a single model. It is generally recommended that redundant contacts, i.e., two or more contacts producing forces due to the same penetration (for example near a corner), are

avoided, as this can lead to numerical instabilities. To enable flexibility for the user in modelling contact, commercial codes present a number of contact types and a number of parameters that control various aspects of the contact treatment. But, as already stated, unfortunately, there are no clear rules to choose these parameters, depending from user's experience and, in any case, their values are often obtained by means of trials and error iterative procedure.
Anyway, the best way to start a contact analysis by using a commercial explicit solver is to consider default settings for these parameters, even if often non-default values are more appropriate, to define the same element characteristic lengths to model interacting surfaces and, overall, to avoid initial geometrical co-penetrations of contact surfaces.
Thus, the selection of integration time step and of the contact parameters are two important aspects to be considered when analysts deal with simulation of the response of structure to impulse loading.
The last important topic examined in the present section and which can result in additional CPU costs as compared to a run where default parameters values are used, regards shell elements formulation. The most widely adopted shells in commercial codes belong to the families of the Hughes-Liu or of the Belytschko-Tsay shell elements. The second one is computationally more efficient due to some mathematical simplifications (based on co-rotational and velocity-strain formulations), but results in some restriction in the computation of out of plane deformations.
But the real problem is that, in order to further reduce CPU time, analysts generally aims to use under integrated shell elements (i.e. with a single integration point), and this causes another numerical problem, which also arises with under-integrated solid elements. This numerical problem concerns the hourglassing energy: single integration point elements can shear without introducing any energy, therefore an added "numerical energy" is generated to take it into account. High hourglassing energy is often a sign that mesh issues may need to be addressed by reducing element size, but the only way to entirely eliminate it is to switch to formulations with fully-integrated or selectively reduced integration (S/R) elements; unfortunately, this approach is much more time expensive and can be unstable in very large deformation applications, therefore hourglassing energy is generally controlled by considering very regular meshes or by considering some corrective algorithms provided by commercial explicit solvers. In any case, these algorithms ask for an analysts much experienced on their formulation, otherwise other numerical instabilities can arise following their use.

3. Some case studies from manufacturing

Some case studies are now presented to introduce the capabilities and peculiarities of the analysis of structures subjected to impulsive loadings; they are connected with some of the relevant problems of manufacturing and will let the reader to grasp the basic difficulties encountered, for example, when dealing with contact elements which model interfaces. The first one deals with the case of riveted joints and shows how to simulate the riveting operation and its influence on the subsequent bulging coming from an axial load, while the second one comes from metalforming and deals with the stretch-bending process of an aluminium C-shaped beam.

3.1 The analysis of the riveting process

The load transfer mechanism of joints equipped with fasteners has been recognized for a long time as one of the main causes which affect both static resistance as well as fatigue life of joints; unfortunately, such components, which are often considered as very simple, exhibit such a complex behaviour that it is far from being deeply understood and only in recent times the coupling of experimental tests with numerical procedures has let researchers begin to obtain some knowledge about the effects which come from assuming one of the available designs.

Starting from the very simple hypothesis about load transfer mechanisms which are used in the most common and easy cases, a real study of such joints has started just after Second World War, mainly because from those years onward the use of bolted or riveted sheets has been increasingly spreading and several formulae were developed with various means; also in those years the "neutral line method" was introduced to study the behaviour of the whole joint, with the consequence that the need of a sound evaluation of fasteners stiffness and contribution to the overall behaviour was strictly required. A wide spectrum of results and theories have appeared since then, each one with some peculiarities of its own and the analysis of bolted and riveted joints appears now as to be analysed by different methods.

The requirement of a wide range of different studies is to be found in the large number of variables which can affect the response of such joints, among which we can quote, from a general but not exhaustive standpoint:

- ***general parameters***: geometry of the joint (single or several rows, simple- or double-lap joints, clamping length, fastener geometry); characteristics of the sheets (metallic, non metallic, degree of anisotropy, composition of laminae and stacking order for laminates); friction between sheets, interlaminar resistance between laminae, possible presence of adhesive;
- ***parameters for bolted joints:*** geometry of heads and washers; assembly axial load; effective contact area between bolts and holes; fit of bolts in holes;
- ***parameters for riveted joints:*** geometry of head and kind of fastener (solid, blind – or cherry – and self-piercing rivets, besides the many types now available); amplitude of clearance before assembly; mounting axial load; pressure effects after manufacture.

From all above it follows that today a great interest is increasingly being devoted to the problem of load transfer in riveted joints, but that no exhaustive analysis has been carried out insofar: the many papers which deal with such studies, in fact, analyze peculiar aspects of such joints, and little efforts have been directed to the connection between riveting operation and response of the joint, especially with regard to the behaviour in presence of damage.

Therefore, the activity which we are referring to dealt with modelling of the riveting operation, in order to define by numerical methods the influence of the assembly conditions and parameters on the residual stress state and to the effective compression zone between sheets; another aspect to be investigated was the detection of the relevant parameters of the previous operation to be taken into account in the analysis of the joint strength.

As we wished to analyse the riveting operation and its consequences on the residual stresses between plates, the obvious choice was to use a dynamic explicit FEM code, namely Ls-Dyna®, whose capabilities make it most valuable to model high-speed transients without much time consumption.

As a drawback, we know that that code is very sensitive to contact problems and that a finer mesh requires smaller integration time intervals: therefore the building of a good model, parametrically organized in order to make variations of input parameters easy, took a long time. The procedure we followed was to use ANSYS® 10.0 PDL (parametric design language) capabilities to be coupled with Ls-Dyna solver to obtain a global procedure which can be summarized in the following steps:

- Write a parametric input file for ANSYS PDL, where geometry, behaviour of materials, contact surfaces and conditions, load cases were specified; it gives a first approximate and partially filled Ls-Dyna input file;
- Complete the input file for Ls-Dyna, in order to introduce those characteristics and instructions which are required, but which are not present in Ansys code, mostly control cards and some variations on materials;
- Solve the model by Ls-Dyna code;
- Examine the results by Ls-PrePost or by Ansys post-processor module, or by Hyperview® software, according to the particular requirements.

In fig. 1 one can see the basic Ls-Dyna model built for the present analysis, with reference to a solid rivet; the model is composed of seven parts, among which one can count three solid parts, made of brick elements, and four parts composed by shells: three of these are required to represent the contact surface, while the last composes a plane rigid wall that represents the riveting apparatus.

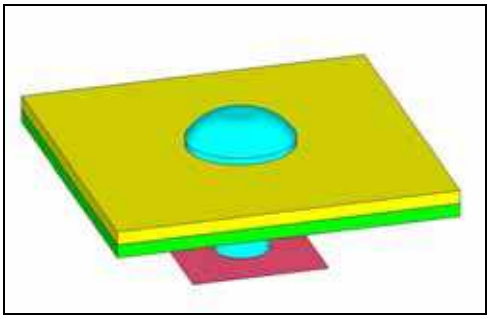

Fig. 1. The model used to simulate the joint

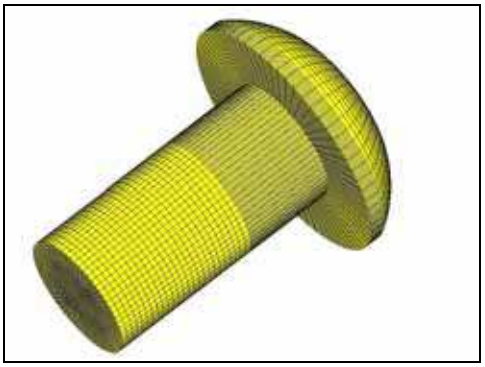

Fig. 2. The model of the rivet

A finer mesh – with a 0.2 mm average length – was adopted to model the stem of the rivet (fig. 2) and those parts of the sheets which, around the hole and below the rivet head, are more interested by high stress gradients; a coarser mesh was then adopted for the other zones, as the rivet head and the parts of the sheets which are relatively far from the rivet.
The whole model was composed, in the basic reference case, of 101,679-109,689 nodes and 92,416-100,096 brick elements, according to the requirements of single cases, which is quite a large number but also in that case runtimes were rather long, as they resulted to be around 9-10 hours on a common desktop; more complex cases were run on a single blade of an available cluster, equipped with 2 Xeon 3.84 GHz - 4 GB RAM - and of course comparatively shorter times were obtained.
The main reason of such times is to be found in the very short time-step to be used for the solution, about 1.0E-08 s, because of the small edge length of the elements.
The solid part of rivet and sheets were modelled following a material 3 from Ls-Dyna library, which is well suited to model isotropic and kinematic hardening plasticity, with the option of including strain rate effects; values were assigned with reference to 2024 aluminium alloy; the shells corresponding to the contact surfaces were then modelled with a material 9, which is the so-called "null material", in order to take into account the fact that those shells are not a part of the structure, but they are only needed to "soften out" contact conditions; for that material shells are completely by-passed in the element stiffness processing, but not in the mass processing, implying an added mass, and for that reason one has to manually assign penalty coefficients in the input file. Some calibration was required to choose the thickness of those elements, looking for a compromise between the influence of added mass – which results from too large a thickness – and the negative effect with regard to contact, which comes in presence of a thickness too small, as in that case Ls-Dyna code doesn't always detect penetration.
The punching part was modelled as a rigid material (mat. no. 20 from Ls-Dyna library); such a material is very cost effective, as they, too, are completely bypassed in element processing and no space is allocated for storing history variables; also, this material is usually adopted when dealing with tooling in a forming process, as the tool stiffness is some order larger than that of the piece under working. In any case, for contact reasons Ls-Dyna code expects to receive material constants, which were assumed to be about ten times those of steel.
For what concerns the size of the rivet, it was assumed to be a 4.0 mm diameter rivet, with a stem at least 8.0 mm long; as required by the general standards, considering the tolerance range, the real diameter can vary between 3.94 and 4.04 mm, while the hole diameter is between 4.02 and 4.11 mm, resulting in diametral clearances ranging from 0.02 to 0.17 mm; three cases were then examined, corresponding to 0.02-0.08-0.17 mm clearances.
The sheets, also made of aluminium alloy, were considered to range from 1.0 to 4.0 mm thickness, given the diameter of the rivet; the extension examined for the sheets was assumed to correspond to a half-pitch of the rivets and, in particular, it was assigned to be 12.5 mm; along the thickness, a variable number of elements could be assigned, but we considered it to be the same of the elements spacing along the stem of the rivet: that was because contact algorithms give the best results if such spacing is the same on the two sides of the contact region. In general, we introduced a 0.2 mm edge length for those elements, which resulted in 5 elements along the thickness, but also case of 10 and 20 elements were investigated, in order to check the convergence of the solution.
At last, for what concerns the loads, they were applied imparting an assigned speed to the rigid wall, and recovering *a posteriori* the resulting load; that was because previous

experiences suggested not to directly apply forces; besides, all applicable loads accepted by Ls-Dyna are body forces, or one concentrated force on a rigid body, or nodal forces or pressure on shell elements: the last two choices don't guarantee the planarity of the loaded end after deformation, which can be obtained by applying the load on the tool, but that use in past experiences revealed to be rather difficult to be calibrated.
Therefore, we assumed a hammer speed-time law characterized by a steep rise in about 0.006 s up to the riveting speed, which remains constant for a convenient time, then subduing an inversion also in about 0.006 s after the wanted distance has been covered; considering that the available data mention 0.2 s as a typical riveting time, the tool speed has been assumed to be 250 mm/s, even if the effects of lower velocities were examined (200, 150 and 50 mm/s).
Therefore, summarizing the analyses carried out insofar, the variables assumed were as follows:

- Initial clearance between the rivet stem and the hole;
- Thickness of the sheets;
- Speed of the tool.

The results obtained can be illustrated, first of all, by means of some countour plots, beginning from fig. 3 and 4, where the variation of von Mises equivalent stress is illustrated for the cases defined above, concerning the clearance amplitude between rivet and hole; it is quite evident, indeed, that the general stress state for the max clearance case is well below what happens when the gap decreases, also considering the scale max values: the mean stress level in sheets increases, as well as the largest absolute values, which can be found in correspondence of the folding of the rivet against the edge of the hole.

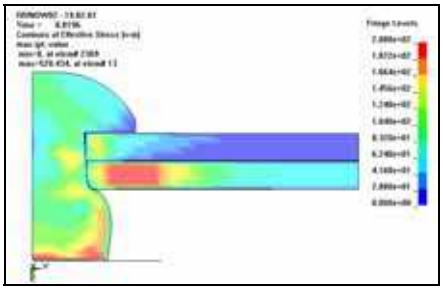

Fig. 3. Von Mises stress during riveting for max clearance

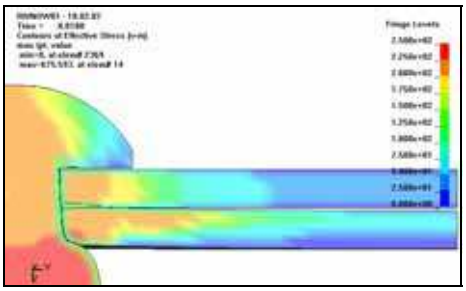

Fig. 4. Von Mises stress during riveting for min clearance

While the previous results have been illustrated with reference to the time when the largest displacement of the rigid wall occurs, others can be best observed considering the final time, when the tool has left the rivet and possible stress recovery determined.
For example, it can be useful to look at the distribution of pressure against the inner surface of the hole for the same cases above. The results observed can be summarized considering that in presence of the max clearance the rivet can fill the hole completely – and that the second sheet is only partially subjected to internal load – and then all the load is absorbed from the first edge of the hole, which is therefore overstressed, as a part of the wall doesn't participate to balance load; also the external area of the first sheet interested by the folding of the rivet is quite large.
When clearance reduces it can be observed that gradually all the internal surface of the hole comes in contact with the rivet and therefore it can exert a stiffening action on the stem, which folds in a lesser degree and therefore can't transmit a very large load on the edge of the hole, as it can be observed in fig. 5 as the volume of the sheet which is subjected to significant radial stresses.

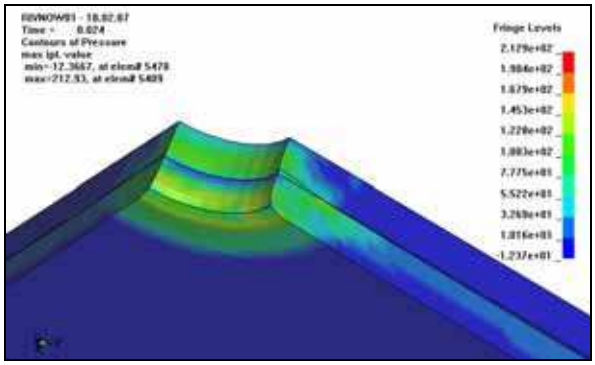

Fig. 5. Residual pressure for min clearance

Also the extension of the volume interested by plasticity increases; in particular we obtained that in presence of a larger gap only a part of the first sheet is plastically deformed, but, at the same time, that the corresponding deformation reaches higher values, all in correspondence of the external edge or immediately near to it; as clearance reduces the max plastic deformation becomes smaller, but plasticity reaches the edge of the second sheet and that effect is still larger in correspondence of the min clearance, where a larger part of the second sheet is plastically deformed; at the same time the largest values of the plastic deformation in correspondence of the first edge becomes moderately higher for the constraint effect exerted by the inner surface of the hole and above noted.
It is interesting to notice that the compression load is no much altered by varying the riveting velocity, as it can be observed from fig. 6 for 1.00 mm thick plates; what is more noteworthy is the large decrease from the peak to the residual load, which is, more or less, the same for all cases.
On the other hand, the increase of thickness produces larger compression loads (fig. 7), as it was to be expected, because of the larger stiffness of the elements. It must be noted, for comparison reasons, that for the plots above the load is the one which acts on the whole rivet and not on the quarter model.

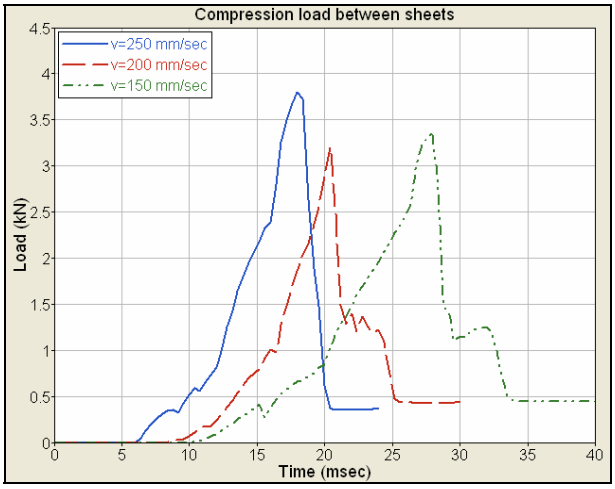

Fig. 6. Influence of velocity on compression load

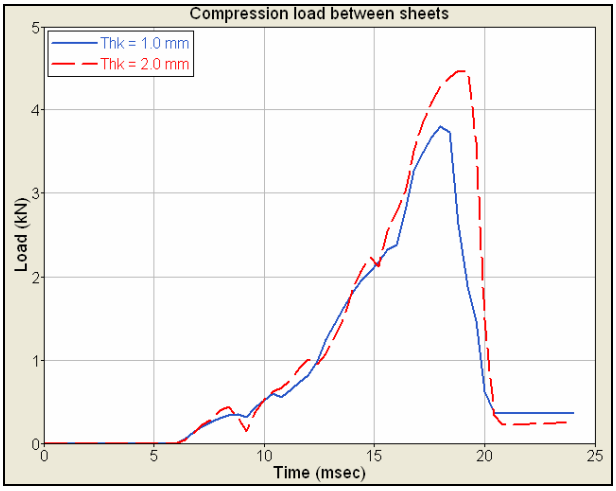

Fig. 7. Influence of thickness on compression load

Aiming to evaluate the consequences of the riveting operation on the behaviour of a general joint, because of the residual stress state which has been induced in the sheets, the effect of an axial load was investigated, considering such high loads as to cause a bulging effect. As a first step, using an apparatus (Zwick Roell Z010-10kN) which was available at the laboratories of the Second University of Naples, a series of bearing experimental tests (ASTM E238-84) have been carried out on a simple aluminium alloy 6xxx T6 holed plate (28.5 x 200 x 3 mm3, hole diam. 6 mm), equipped with a 6 mm steel pin (therefore different from that for which we presented the results in the previous pages) obtaining the response curves shown in Fig. 8. In the same graph numerical results have been illustrated, carried out from non linear static FE simulations developed by using ANSYS® ver. 10 code. As it is

possible to observe the agreement between numerical and experimental results is very good. This experimental activity allowed to setup and develop the FE model (Fig. 9) of each single sheet of the joint and, in particular, their elastic-plastic material behaviour.

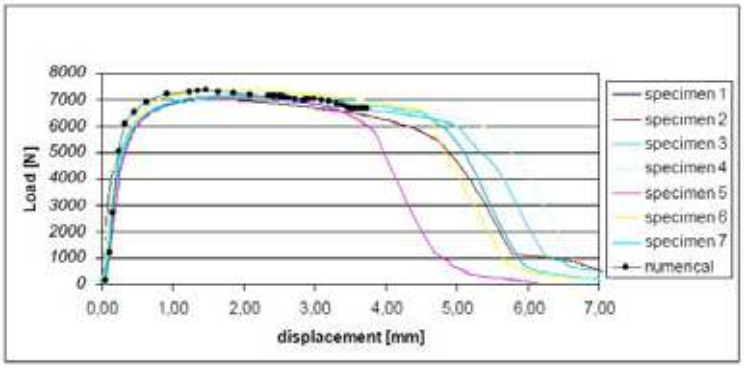

Fig. 8. Results from experimental and numerical bearing tests

Fig. 9. FE model of a single joint sheet

In order to investigate on the influence of the riveting process, the residual stress-strain distribution around the hole coming from the riveting process above was transferred to the model of the riveted joint (sheets dim. 28.5 x 200 x 1 mm3, hole diam. 6 mm). The transfer procedure consisted in the fitting of the deformed rivet into the undeformed sheets and in the subsequent recovery of the real interference as a first step of an implicit FE analysis.
After the riveting effect has been transferred to the joint the sheets were loaded along the longitudinal direction and the distribution of Von Mises stress around the hole of one sheet of the joint in presence of the maximum value of the axial load value is illustrated in Fig. 10. The results in terms of axial load vs. axial displacement have been compared (Fig. 11) with

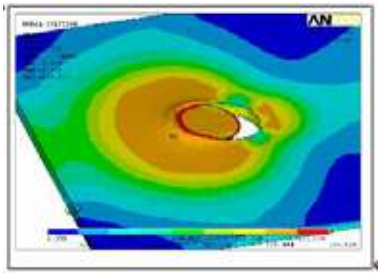

Fig. 10. Bulging of the riveted hole coming from implicit FEM

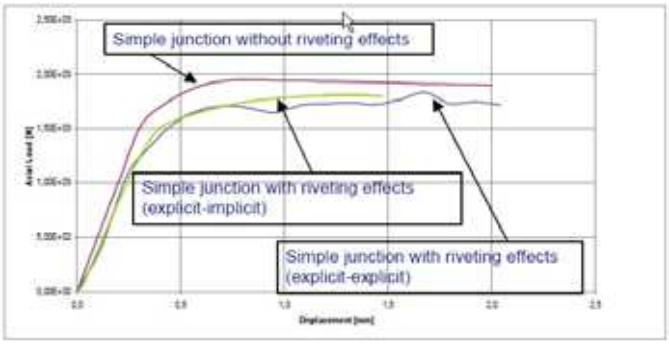

Fig. 11. Effect of the residual stress state on the behaviour of the joint

those previously obtained from the analysis of the same joint without taking into account the riveting effect: it is possible to observe that the riveting operation effects cause a reduction of the bearing resistance of the joint of about 10%. On the same plot also the results obtained by analysing also the axial loading by means of the explicit codes are illustrated: this procedure obviously proved to be very time consuming compared to the use of an explicit to implicit scheme, without giving relevant advantages in terms of results and therefore it is clear that the explicit-implicit formulation can be adopted for such analyses.

3.2 A stretch-bending case study

As it is known, the space frame with the whole load-carrying structure made of aluminium alloy is an assessed concept. A feature of this kind of application is that the originally straight extrusion of some component must be followed by some plastic forming operations in order to obtain the desired shape/curvature. Several types of modified bending processes are thus introduced, e.g. press bending, rotary draw bending, stretch bending, etc.

Typical concerns regarding the industrial use of these methods are the magnitude of the tolerances during production and the cross-sectional distortions of the curved specimen. The tolerance problem is primarily related to the springback phenomenon: springback is the elastic recovery taking place during unloading; the most important cross-sectional distortions are local buckling in the compression zone and sagging, which is a curvature-induced local deformation of the cross-section.

In-house experience combined with trial-and-error procedures has been the traditional solution of the tolerance and distortion challenges in industrial bending. This approach may be time consuming and expensive, therefore alternative methods are requested, including the use of the numerical simulation by means of finite element method.

There are several difficulties associated with a numerical simulation of the stretch bending of extruded components; the main ones are non-linear material behavior, geometrical non-linearities, modeling of boundary conditions, contact between die and specimen, springback during the unloading phase. Another very complex aspect is the calibration of the numerical model as rather few experimental results are available in the literature. In any case, to simulate these typologies of phenomena explicit FE algorithms can be certainly considered the most suitable, for what concerns both the computational efficiency and the solution accuracy; on the other side, implicit FE algorithms can be considered in the most of applications more effective in the spring-back phase.

The experimental test-case regards a process of stretch-bending of a single frame (3000 mm length) of aluminium alloy 7076, whose transversal section is represented in figure 12; during the process the ends of the frame are clamped and a tensile force, corresponding to the yield force or somewhat higher, is applied to the specimen. Then the frame is bended by fitting it around a die (3300 mm radius) with the mandrel fixed and the arms of the machine rotating. Stretch bending of the frame has been developed after it has been subjected to a quenching treatment.

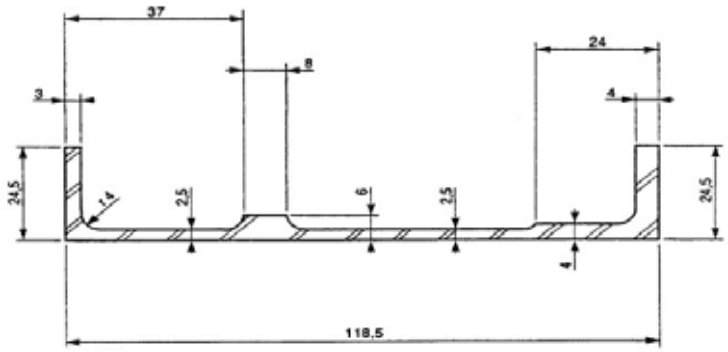

Fig. 12. Transversal section of the bended frame (dimensions are in mm)

In order to evaluate residual stresses after the stretch bending, experimental hole-drilling measurements have been performed in opportune locations on the frame, as showed in figure 13, where also the test apparatus is illustrated.

Fig. 13. Hole drilling measurement locations and test apparatus

The developed FE model consists of 743,000 8-noded hexahedral solid elements (3 dof's per node) and 694,000 nodes. Plastic-kinematic behavior is assumed to model mechanical material properties (E=74000 MPa, v=0.3, σ_y=461 MPa, Etan=700MPa). Only half frame has been modelled because of the symmetry. Some solid elements fit into the frame section have been considered in both the real and the virtual process in order to prevent the sagging deformation due to the buckling of the section.

The stretch bending process has been simulated by considering the mandrel fixed in the space and perfectly rigid. The nodes on the transversal section of the frame belonging to the symmetry plane are constrained to move only in the symmetry plane; the nodes of the end transversal section are rigidly linked to the node of the rigid bar elements representing the arms of the bending apparatus, which rotate and push the frame on the mandrel by following opportune paths. It should be noted that the frame is initially stretched and then

bended. The explicit FE algorithms implemented in the Ls-Dyna® [6] code have been used to develop the loading phase of the analysis.
For what concerns the unloading phase, some attempts have been made to solve it by using implicit algorithms of the Ls-Dyna® code, but a lot of convergence problems have been arisen due to the large relative displacements between the different elements of the chain; to avoid this kind of problems significant model modifications are needed, therefore it has been more convenient to simulate the unloading phase by using explicit finite element algorithms, by introducing a fictitious damping factor. In figure 14, the kinetic energy of the frame vs. process time is showed, where it is possible to individuate the start time of the spring-back phase.

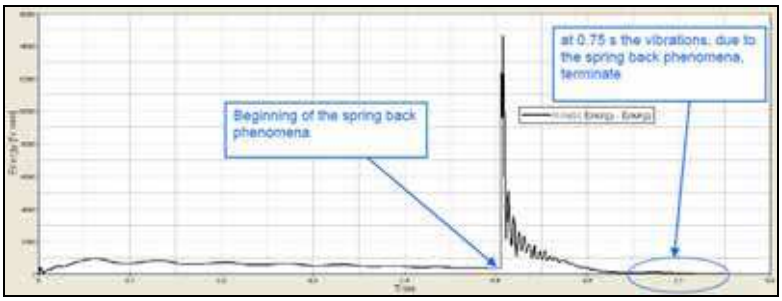

Fig. 14. Kinetic energy of the frame during stretch-bending

4. Biomechanical problems in crashworthiness studies

One of the most relevant issues in today engineering is that related to safety in transportation; as it is a common statement that our lines are as safe and able to avoid any accident in the highest degree, with respect to the actual design and manufacturing procedures, the greatest attention is now being paid to the protection of passengers when unfortunately an impact occurs (i.e. to what is today called the "passive safety").
In those occasions, indeed, passengers can be injured or even killed because of the high decelerations which take place or because they move in the vehicle and impact against the structure or even because the deformation of the structure is so severe as to reduce or even to cancel the required space of survival.
That knowledge has brought designers to introduce sacrificial elements in the structures, i.e. some elements which adsorb the incoming kinetic energy by deformation and slow down decelerations, thus preventing the passengers from severe impacts; in other cases, means restraint such seatbelts are provided, in order to avoid undesired or dangerous motions of the same travellers.
The studies of such dangerous events have shown that the impact occurs in a very short time (typically, 100-150 ms in the case of cars) which explains the large inertia forces which are developed and therefore the analyses have to be carried out in time, i.e. as a transient analysis in presence of finite deformations and of highly non-linear and strain rate dependent materials.
As the aim of such studies is to prevent or at least to limit the damage of passengers, it is obvious that all results are made available in terms of decelerations and impact forces on human bodies, which are to be compared with the respective admissible values, which have

been studied for many years now and are rather well assessed. Specialized centres, as NCAP in the car field, have defined many biomechanical indexes which can now obtained for a given crash scenario from the same numerical analysis of the impact and which can immediately compared with known limit values. For example, the most well known index, HIC (Head Injury Criterion), evaluates the maximum acceleration level which acts for a sufficient time on the neck of a passenger implicated in an accident, according to the following expression:

$$HIC = max\left\{\left[\frac{1}{t_2 - t_1}\int_{t_1}^{t_2} a(t)\cdot dt\right]^{2.5}\cdot(t_2 - t_1)\right\} \tag{12}$$

where a(t) is the total acceleration of the neck which occurs in the interval $t_1 \div t_2$, which usually is assumed to be 36 ms; as that span is shorter than the crash, a window is moved along the time axis up to the point where the largest values of the index are obtained.
Beside HIC, many other indexes have been defined, as VC (Viscous Criterion), TTH (Thorax Trauma Index), TI (Tibia Index) and others, all referring to different parts of the human body; all results are then combined to assess the safety level of the structure (car, train or other) in a particular impact scenario.
The soundness of a structural design which involves safety issues is assessed on that basis and that let us realize the difficulties of the procedure. Beside, one has to realize that the characteristics of the adopted materials have to be precisely known for the particular accident one has to analyze; that means that the behaviour of the materials has to be acquired in the non-linear range, but also in presence of high strain rates. Usually those behaviours are not known in advance and therefore specific tests have to be carried out before the numerical analysis.
At last, because of the simplifying hypotheses one introduces inevitably in the numerical model, it is necessary to calibrate it with reference to some known beforehand particular scenario, to be sure that the behaviour of the material is well modelled.
It has to be stressed that in the past the main way to obtain reliable results was to carry out experimental tests, using anthropomorphic dummies and structures, which suffered such damages as to prevent their further use. That way was very time consuming and implied such unbearable costs that it couldn't be performed on a large scale basis, to examine all possible cases and to repeat test a sufficient number of times; the consequence was that passive safety didn't advance to high standards.
When numerical codes improved to such levels as to manage complex analyses evolving in time in presence of finite stresses and strains, it was only a matter of time before they began to be used to simulate impact scenarios; that has resulted in a better understanding of the corresponding problems and in obtaining a much larger number of results, which in turn allowed an important level of knowledge to be achieved.
Therefore, today activity in passive safety studies is mainly performed by simulation methods and a much lesser number of experimental tests is carried out than in the past. Thus, it is now possible to study very particular and specific cases, but in order to obtain reliable results it is quite necessary to calibrate each analysis with experimental tests and to comply with codes and standards which were often devised when today computers were not yet available.

5. Case studies from crashworthiness analyses

5.1 An example of crashworthiness analysis in the automotive field

In the first development stages of the numerical analysis of vehicle impacts, with studies about the energy absorption capabilities of sacrificial elements and on biomechanical damages, some scenarios were introduced and their understanding deepened, as frontal impact with or without offset, lateral impact, rollover, pole impact and so on.

Those cases are now widely assessed and more particular scenarios are being studied, as that referring to pedestrian impact or that considering the oblique impact against road guardrails; in the present section, however, we introduce a very specific and interesting case, as it can be usefully adopted to clarify the degree of accuracy that is required today.

One of the most interesting cases, indeed, is that referring to the contingency that a passenger, because of his motion in the course of an accident, impacts against one of the fixtures which define the compartment or the many appliances and gadgets which are fitted to its walls or which constitute its structure.

As the most dangerous case is that when it is the passenger's head to be involved in such an impact, the corresponding study is a very relevant one, as one would have to ensure that interior tapestry and its thin foam stuffing, for example, have such energy absorption capabilities as to prevent severe damages to the head when coming into contact with the metal structure of the compartment.

As one of the main advantages of numerical simulation is to reduce the number of physical tests, it is just natural to try and reproduce the experimental conditions and equipments in order to ensure a reliable correlation between the two cases; now, tests are performed on the basis of USA CFR (Code of Federal Regulations), which have been more or less included in EEVC (European Enhanced Vehicle Safety Committee) standards and therefore one has to be sure to comply with them.

The experimental test of such impact is carried out by simply firing a head-shaped impactor against the target in study, hitting it in precisely defined locations along assigned trajectories; such an impactor is just the head of a dummy whose characteristics have to be verified according very strict standards. For example, the head is to be dropped from a height of 376 mm on a rigidly supported flat horizontal steel plate, which is 51 mm thick and 508 mm square; it has to be suspended in such a way as to prevent lateral accelerations larger than 15g to occur and the peak resultant acceleration recorded at the locations of the accelerometers mounted in the headform have to be not less than 225g and not larger than 275g (Fig. 15).

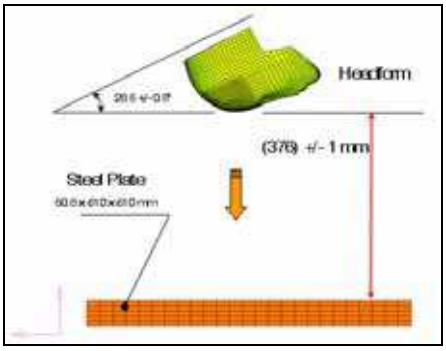

Fig. 15. Headform test conditions

Those standards have hard consequences for the numerical simulations, as one wishes to model the headform as an empty shell-like body, in order to save runtime, but it has to exhibit a stiffness as well as inertia properties such as to be equivalent to the physical head. To respect those conditions and to prevent some wavy dynamic deformations to appear, it can be useful to provide the model with a very stiff ring in the rearmost part (Fig. 16).

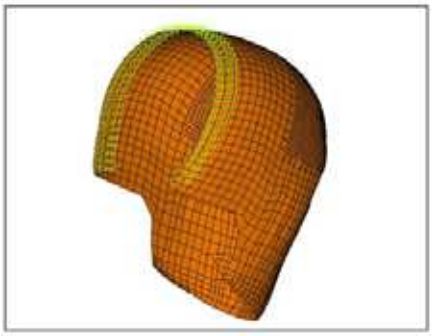

Fig. 16. The stiffened headform

Furthermore, to save time the simulation can start at the time when the impact begins, imparting to the model the same velocity which it would get after falling from the assigned height (Fig. 17). After successfully running the model, an acceleration/time plot is obtained, where the peak values fall in the expected range (Fig. 18).

Once the model of the head has been created and calibrated, one has a large number of difficulties to take into account; beside dashboard, sun visor, header, seat-belt slit, internal handles, there are A- and B-pillars, front header, side rails, and each can be impacted in several points in dependence of the initial position of the passenger. CFR and EEVC show how to define all such points, by means of rules which take into account the geometry of the compartment.

When one comes to a particular obstacle, one has to consider that it is not an easy, single part component; broadly speaking, it is composed by a padding which is mounted on the structure with the interposition of a foam stuffing and the padding usually has several ribs which stiffen the component and position it exactly on the structure. Moreover, the mounting can be obtained by adhesives, clips, rivets or by other means. All that has to be

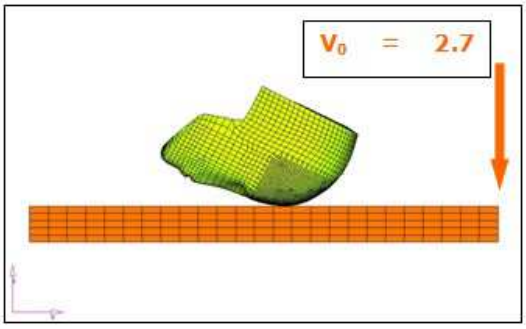

Fig. 17. Imparting an equivalent velocity to the headform

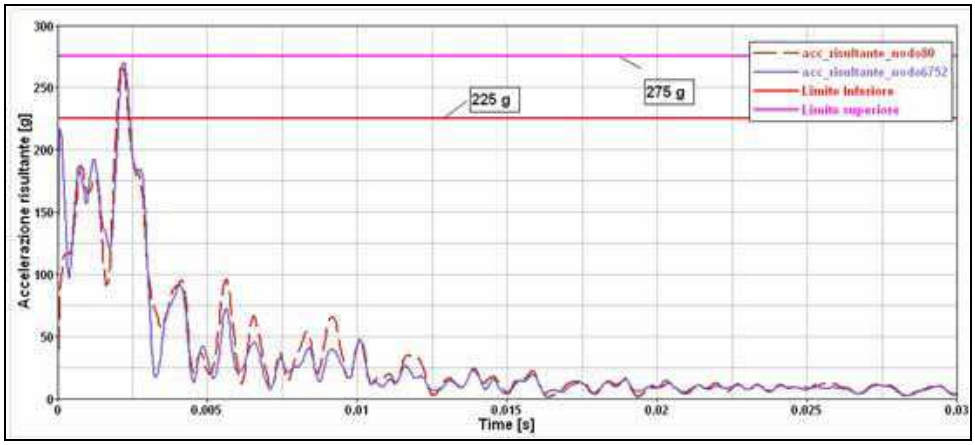

Fig. 18. Resultant acceleration in dropping test

modelled precisely if one wants to get reliable results and beside the modelling elements one has to add the interface ones, which are elements such as to take into account the contact conditions and to prevent copenetrations between the different bodies.
The result is that the modelling task is not at all a secondary one, but it requires a long labour and great attention, also because of the particular shapes which characterize today the various components.
For example, in Fig. 19 it is shown the case of the simulation of the impact of the headform against an upper handle; the use of a code like Ls-Dyna® let the analyst get a complete set of results, such as displacements, velocities and accelerations of each element, as well as contact and inertia forces, beside the energy involved, subdivided in all relevant parts, as kinetic, deformation, and so on.

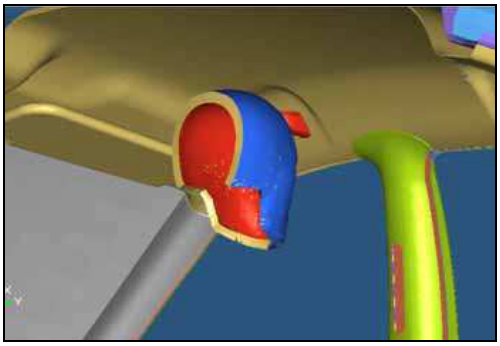

Fig. 19. The impact of the headform against the internal upper handle

Nevertheless, one has to realize that the obtained results are not so smooth as one could guess, because of evaluation and round-off errors, instability of the elements and of the numerical procedure, and so on; once grouped in a plot, the result curves show peaks and valleys which are meaningless and have to be removed, just as one does when dealing with vibration or sound curves; the usual technique is to treat the numerical values with a filter (for example, SAE 100 or 180) which makes the plot more intelligible.

One of the obtained results, for example, is that shown in Fig. 20, which refers to the previous impact case against the handle; four curves are shown, i.e. the experimental one, together with ±15% curves, which bound the admissible errors, and that which comes from numerical simulations; as it can be observed, the numerical values are all inside the admissible range, but for a later time, which comes when the headform has left the obstacle and is moving free in the compartment, which is of no interest.

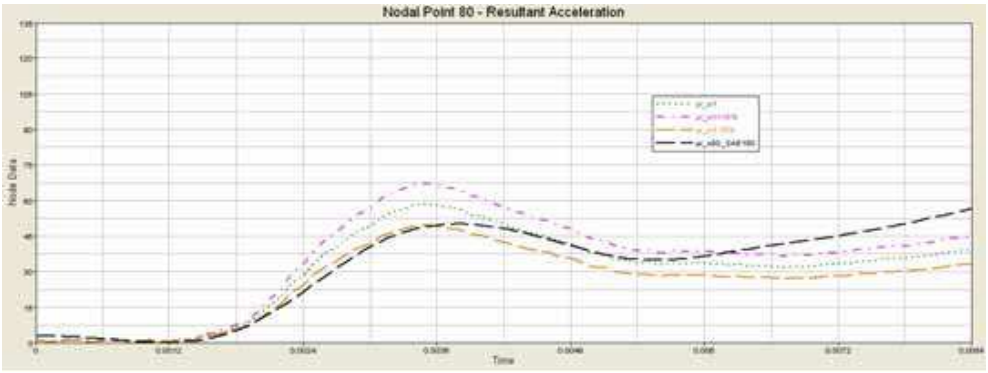

Fig. 20. Resultant acceleration for the impact of the headform against the internal upper handle

5.2 Crashworthiness analyses in railways

The survival of the occupants of a railway vehicle, following an accident, depends substantially from three aspects:

- type and severity of the accident;
- crash behaviour of the structure as a whole;
- resulting type and severity of secondary impacts which occur because of the relative speed between passengers and interiors.

The investigation on these aspects, by means of numerical methods, starts from the identification and the successive simulation of opportune impact scenarios involving a detailed numerical model of the vehicle as a whole. The identification of the most representative impact scenarios is taken from the EN15227 standard (Railway applications - Crashworthiness requirements for railway vehicle bodies). The simulation of the impact scenario provides the evaluation of the deformations suffered from the structure and from the interiors and allows the identification of the kinematic and dynamic properties necessary to set up the biomechanical analyses.

Within this work, the overall resistance of the vehicle was considered fixed, as the mean objective was the simulation of the biomechanical performances of an interior component (hereinafter also called panels), in order to identify its characteristics of passive safety and to assess guidelines to improve its design.

The goal was to set up a hybrid methodology which uses in a combined way FEM to extract the effective dynamic and structural behaviour of the interiors, and the multibody method (MB) to determine the kinematic of secondary impacts and biomechanical parameters. It has to be pointed out that when one is not interested to internal stress and strain states coming from a dynamic phenomenon, a different method can be used, the multibody one, which is

very fast and efficient and which can be coupled with a FEM analysis when completing the study.

The steps followed to develop this activity are listed below:

1. obtaining by FEA the "pulse" necessary to initialize the multibody analysis: within this phase the dynamic behaviour of the interiors have been also evaluated;
2. obtaining by MB analysis the kinematic behaviour of passengers;
3. obtaining contact stiffness of the interiors by local FE analyses, which has been used to characterize the stiffness of the panels in the multibody environment;
4. simulating the secondary impacts in a multibody environment.

According to the EN15227 standard, the selected collision scenario has been the frontal impact between two similar vehicles (Fig. 21) at a speed of 36 km/h; such scenario has been modelled and analyzed, by using the explicit finite element code LS-Dyna®, as a collision of a single vehicle against a rigid barrier at a speed of 18 km/h.

Fig. 21. The FEM model of a train coach

The first phase of the analysis has regarded the estimation of the deformations of the vehicle as a whole, with the aim to evaluate the reduction of the occupants/driver survival space and the probable disengagement of the bogie wheels from the rail. Stated the respect of these standard requirements, the successive phase has regarded the analysis of the energies involved in the phenomenon (Fig. 22); the value of the initial kinetic energy of the vehicle is 851,250 J, which at the end of the impact is fully converted into internal energy of the system. It should be considered that the internal energy includes the elastic energy stored by the buffer spring, which is recovered in terms of kinetic energy during the "bounce" of the vehicle. As it can be seen in Fig. 22, about 50,000 J are absorbed in the first phase of the impact by the buffer; once the buffer spring has been fully compressed, about 600,000 J are absorbed by the two absorbers, proportionally to their characteristics.

The next analyzed resulting parameter is the acceleration, which in this case has been evaluated on the “rigid” pin linking the structure to the forward bogie. As it can be seen from the plot in the lower left of Fig. 22, which will be the "pulse" for the Multibody analysis, during the absorption of the impact energy by the buffer/absorbers group, the maximum acceleration value is about 5g, to grow up to about 15g when the frame is involved in the collision.

Finally, it has been evaluated the interface reaction between the vehicle and the barrier (Fig. 22): it is almost constant, with acceptable maximum value, until the frame is involved in the collision.

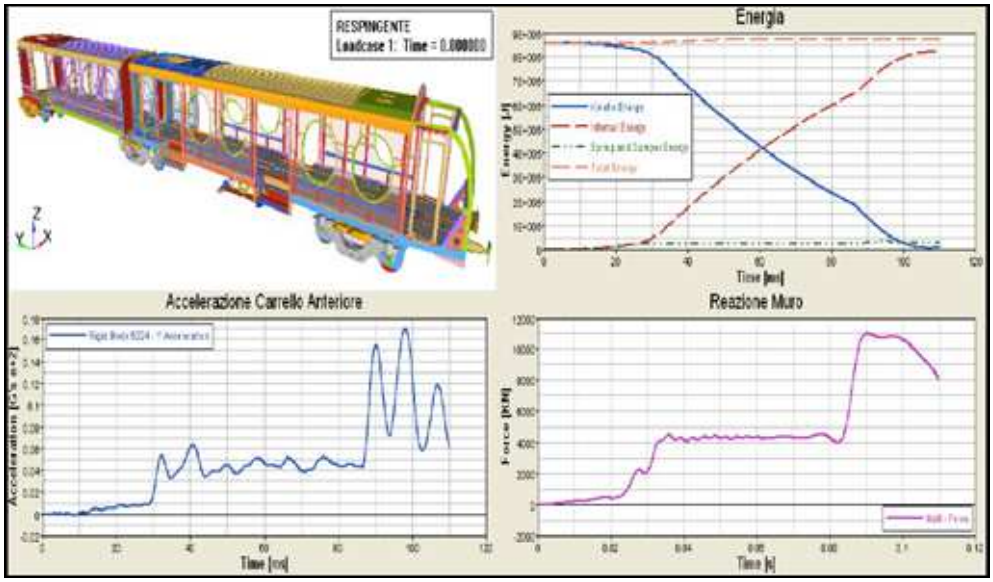

Fig. 22. Pulse evaluation from FEM analysis

The main objective of the work is to develop a complete multibody model of a critical area inside a train unit, including the model of an anthropomorphic dummy, which allows to develop fast simulations of secondary impact scenarios from which to obtain biomechanical results; moreover, by proceeding in this way, it is also possible to quickly evaluate the changes in biomechanical performances of the interiors that characterize different configurations (stiffness of the panels, thickness and arrangement of the reinforcement, etc.).
In order to characterize the contact reaction between the dummy and the interiors in a multibody environment, the panels are modelled as rigid bodies, but their impact surfaces react to the impact by following an assigned law of the reaction forces vs. displacement through the contact surface. This law must be evaluated either by considering experimental compression tests of the panel, or by developing a local finite element analysis by modelling the real properties of the materials of the panels.
The advantages in the use of this hybrid methodology are briefly described below:

- a full multibody model (free from FE surfaces) requires very short calculation time;
- the multibody model is a very flexible one, in which it is possible to change the "response of the material" by acting only on the characteristics of stiffness at the contact interface;
- the change in geometry of the multibody model is very simple and fast.

In Figs. 23 and 24, we show some images related to the preliminary multibody analysis performed by using Madymo® MB commercial code, by considering as perfectly rigid the surfaces representing all the components of the considered scenario. This analysis provides information about the kinematic of the secondary impacts involving a generic seated passenger (Dummy "Hybrid_III_95% ile") and a composite panel positioned in front of him. We also introduced the hypothesis that the effective stiffness of the impacted panels doesn't influence the relative kinematic between the panels and the passengers.

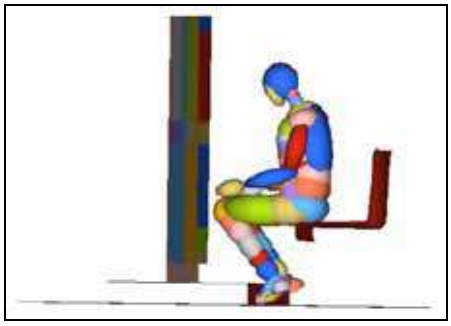

Fig. 23. 140 ms, the dummy breaks away from the seat; feet are blocked under the step and are not able to slide on the floor.

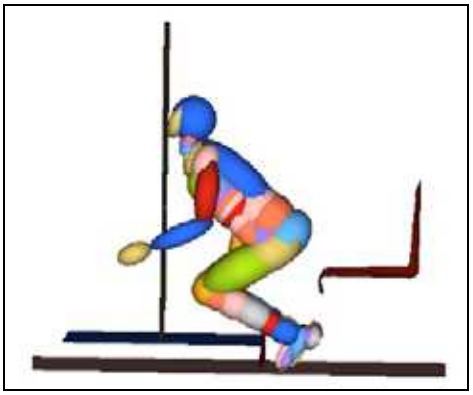

Fig. 24. 235 ms: the neck reaches the critical position: this is the maximum deflection

From this preliminary analysis it was possible to extract information about the exact areas of the panels interested from the impact with the passenger; the next step was to develop a explicit finite element analysis in order to evaluate the effective "contact stiffness" of these areas.

To evaluate by explicit FE analysis the effective stiffness of the interior panels it is not useful to consider a sub-model of the areas of the whole panel interested from the impact, because of the effective local stiffness depends on the effective boundary conditions, in terms of type and position of the constraint and of the stiffeners positioned beside the panel.

For what concern the dummy, in the finite element analysis it has been replaced by a series of rigid spherical bodies, with an opportune calibrated mass (19 kg for knee and 9.6 for the head) and with a specific speed (5 m/s), in order to obtain the same impact energy value. The impact areas were chosen considering the kinematic analysis made previously and in particular they have been chosen considering the knees and the head impact areas.

For every collision were considered 4 cases for the knees impacts, and 4 cases for the head impacts, two of which are showed in figures 25 and 26. From those analyses it has been possible to obtain the effective stiffness of the panels to set up the "contact stiffness" of the multibody ones.

Fig. 25. Comparison between contact forces in Dyna-Madymo in the head area

Fig. 26. Comparison between contact forces in Dyna-Madymo in the area of the SX knee

The thus obtained contact stiffness was used to characterize the panels and a multibody analysis was developed in order to obtain the biomechanical indexes. To evaluate different scenarios of secondary impact, some changes to the initial model were considered; the changes concern:

- replacing of the step on the floor by a ramp;
- changing the position of the seat by the maximum distance from the panel.

The results obtained from the full multibody analysis are reported in terms of the biomechanical indexes characterizing the impact scenarios described in the previous section. In Tab. I the biomechanical indexes related to the head are reported; in the last column the limit values are illustrated for each index.

Following the previous analysis it was possible study the 'best' configuration of the interiors in order to limit damages to passengers during the secondary impact; for example, it was possible to confirm that the best configuration was that where the step was no longer present and the seat had the maximum distance from the panels.

Biomechanical indexes	With step	Without step, Seat in a rearward position	Advanced position	Limit of value
Head Injury Criterion (36ms)	**5865.1**	**2866.0**	**2540.9**	500
Resultant head acceleration (3ms,cumulative)	**270.6** (m/s^2)	**1372.9** (m/s^2)	**1888.0** (m/s^2)	800 (m/s^2)
Normalized neck injury criteria	**2.402**	0.436	0.768	1
Viscous criteria	4.301E- 03(m/s)	4.100E-02 (m/s)	0.216 (m/s)	1(m/s^2)

Table I Numerical values of the obtained biomechanical indexes

5.3 Crashworthiness analyses in aeronautics

This work deals with a numerical investigation about the most reliable procedure to simulate, by finite element method, a sled-test to certificate aeronautical seat. These types of tests are mostly characterized by strongly dynamic effects, even if some evaluations about structural behaviour under quasi-static load conditions are required to certificate the seat. Generally, to develop numerical analyses of dynamic behaviour, explicit finite element algorithms are used; to develop quasi-static analyses both explicit and implicit methods could be suitable. Comparisons between results carried out by using both the methods have been developed, in terms of accuracy of results, calculation time and feasibility of preprocessing phase.

As a reference case we choose an archetype of a passenger seat of an helicopter which is comprised in the "Small Rotorcraft" category, as defined by EASA CS-27 standard. The numerical simulation refer to the "test 2 AS8049 SAE" which states that the seat (dummy included) is subjected at first to a displacement set such as to represent the effect of the deformation of the floor, in quasi-static conditions, then an assigned velocity is impressed to it and at last it is stopped according to a prescribed deceleration curve. It is then possible to identify two distinct phases in the test, the first being characterized by quasi-static phenomena (pre-crash) and the second one accompanied by largely dynamical phenomena (crash).

As the advantages of explicit FEM of the crash phase are well known, the attention was focused on the analysis methods of quasi-static phenomena which characterize pre-crash phase and which in our case are as follows:

- the introduction of rotation of the seat mounting to simulate the effect of the deformation of the aircraft floor;
- the positioning of the dummy and the simulation of the subsequent crushing of the set foam.

The aim of the whole procedure was to find out the most convenient analysis conditions to simulate pre-crash phase, for what refers to reliability of results, computational weight and user-friendliness of preprocessing.

According to AS 8049 SAE standard, a minimum of two dynamical tests is required to certificate the seat and the restraining system, which have both to protect the passenger in the crash phase. On the present work, the test no. 2 was simulated, which considers that a 12.8 m/s velocity is impressed to the seat, which is mounted on a sled, after subduing quasi-static deformations, and which is then stopped in 142 ms, according to a triangular deceleration profile. The inertia forces resultant is directed along a 10° direction with respect

to the longitudinal axis of the aircraft, because of the presence of the main component, which is directed along the longitudinal axis of the aircraft.
The effect of the floor deformation was simulated by applying assigned rotations to the links of the seat to the aircraft structure, which generally occurs through rails which are called "seat tracks". Pitch and roll beam angles, thus simulating the behaviour of the seat-tracks, are assumed to be 10°, and their direction is such as to simulate the hardest load condition.
The two rotations occur in 100 ms each, according two functions whose behaviour can be subdivided in three intervals, as follows:

- increasing velocity according a linear law, from 0 to 2.627 rad/sec;
- constant velocity, at 2.627 rad/sec;
- deceleration, according a linear law up to stop.

The procedure was carried by using the commercial code RADIOSS which let the user choose between explicit and implicit integration; that capability was very useful in this case, because explicit codes require very long runtimes when analyzing quasi-static conditions. In Fig. 27 the results are shown for both explicit and implicit analysis of the connection substructure between the seat and the floor, as appearing after a 10° rotation of the junction between the right leg and the floor; it can be seen that the results are almost the same for the two formulations.

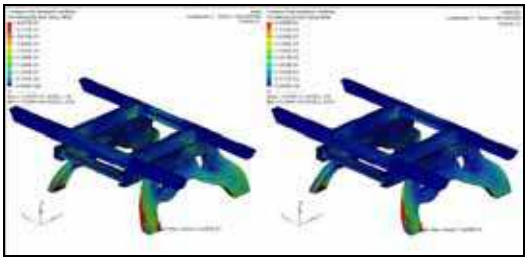

Fig. 27. Von Mises stress as obtained through the explicit (left) and implicit (right) methods

As the object of this paper was the evaluation of the behaviour of the seat, neglecting for the time being the analysis of the passenger, the latter could be simulated by means of a simplified dummy, which could be a rigid one, without joints, with the whole mass was concentrated in its gravity center. A second rigid body was introduced to simulate the whole structure of the seat, but for the elements which represent the two cushions; that behaviour doesn't invalidate the procedure and let reduce greatly the subsequent runtimes.
In the following Fig. 28 we represented the plot of the vertical displacement of the gravity center of the dummy and the kinetic energy of the system as functions of time; the max displacement (6.36mm) is the same for both formulations (implicit and explicit).
After the previous analyses, a complete run for the whole certification test was carried out through an explicit code. In Fig. 29 we have the plots of energy, velocity and acceleration which refer to the master nodes of the rigid elements which simulate the connection between the seat and the floor. For what refers to the kinetic energy, we can observe a point of discontinuity after 200 ms from the beginning of the test: it corresponds to the separation point between the quasi-static phase and that highly dynamic of crash phase. The peak value of kinetic energy appears just at the beginning of crash and amounts to 7680 J, i.e. the total energy of the whole system, whose mass is 93.75 kg, when its velocity is 12.8 m/s.

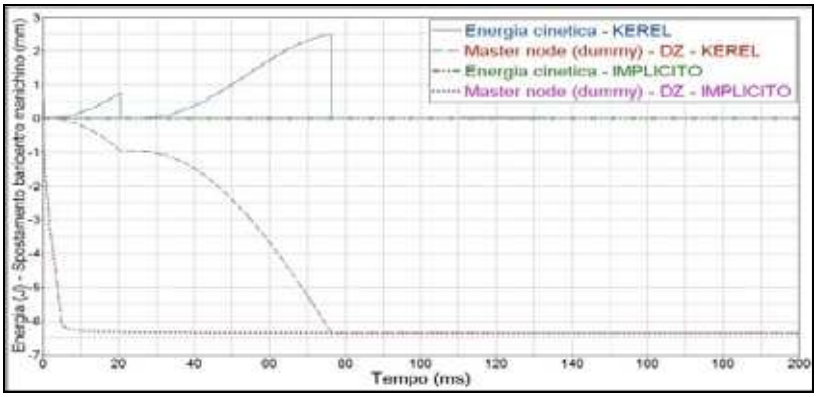

Fig. 28. Vertical displacement and Energy of the gravity center of the dummy

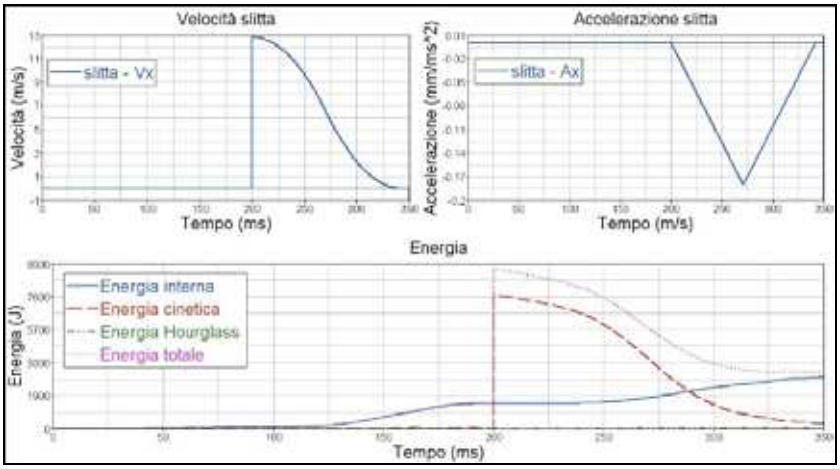

Fig. 29. Velocity and acceleration of the sled, with the absorbed Energy levels

6. Conclusions

Today available explicit codes allow the analyst to study very complex structures in presence of impulsive loads; the cases considered above show the degree of deepening and the accuracy which can be obtained, with a relevant gain in such cases as manufacturing, comfort and safety.

Those advantages are in any case reached through very difficult simulations, as they require an accurate modeling, very fine meshes and what is more relevant, a sound knowledge of the behaviour of the used materials in very particular conditions and in presence of high strain rates.

The continuous advances of computers and of methods of solution let us forecast in the near future a conspicuous progress, at most for what refers to the speed of processors and algorithms, what will make possible to perform more simulations, yet reducing the number of experimental tests, and to deal with the probabilistic aspects of such load cases.

7. References

Chang, J.M.; Tyan, T.; El-bkaily, Cheng, M.J.; Marpu, A.; Zeng, Q. & Santini, J. (2007), Implicit and explicit finite element methods for crash safety analysis, *Proceedings of World Congress Detroit, Michigan;* SAE, Warrendale, Pa.;

Clausen, A.H.; Hopperstad, O.S. & Langseth, M (2001). Sensitivity of model parameters in stretch bending of aluminium extrusions, *J. Mech. Sci.* Vol. 43, p. 427. doi:10.1016/S0020-7403(00)00012-6

Dias, J.P. & Pereira, M.S. (2004). Optimization methods for crashworthiness design using multibody models, *Composite & Structures*, vol 82, pp. 1371-1380, ISSN 0263-8223;

Drazetic, P.; Level, P.; Cornette, D.; Mongenie, P & Ravalard, Y. (1995). One-Dimensional modelling of contact impact problem in guided transport vehicle crash, *Int. J. Impact Engng*, vol 16/3, pp 467 – 478, ISSN 0734-743X;.

European Standard EN 15227 (2008). Railway applications - Crashworthiness requirements for railway vehicle bodies;

Fitzgerald, T.J. & Cohen, J.B. (1994). Residual Stresses in and around Rivets in Clad Aluminium Alloy Plates, *Materials Science & Technology*, vol. AI88, pp. 51-58, ISSN 0267-0836;

Kirkpatrick, S.W.; Schroeder, M. & Simons, J.W. (2001). Evaluation of Passenger Rail Vehicle Crashworthiness, *International Journal of Crashworthiness*, Vol. 6, No. 1, pp. 95-106, ISSN 1358-8265;

Kirkpatrick, S.W. & MacNeil,R.A. (2002). Development of a computer model for prediction of collision response of a railroad passenger car, *Proceedings of the 2002 ASME/IEEE Joint Rail Conference*, pp. 9 - 16, Washington, DC, April 23-25; ISBN 0-7918-3593-6.

Kradinov, V.; Barut, A.; Madenci, E. & Ambur, D.R. (2001). Bolted Double-Lap Composite Joints under Mechanical and Thermal Loading, *Int. J. of Solids & Structures*, vol. 38, pp. 7801-7837, ISSN 0020-7683;

Langrand, B.; Patronelli, L.; Deletombe, E.; Markiewicz, E. & Drazétic:, P. (2002). Full Scale Characterisation for Riveted Joint Design, *Aerospace Science & Technology*, vol. 6, pp. 333-342, ISSN 1270-9638;

Langrand, B.; Fabis, J.; Deudon, A. & Mortier, J.M. (2003). Experimental Characterization of Mechanical Behaviour and Failure Criterion of Assemblies under Mixed Mode Loading. Application to Rivets and Spotwelds, *Mécanique & Industries*, vol. 4, pp. 273-283, ISSN 1296-2139;

Madenci, E.; Shkarayev, S.; Sergeev, B.; Oplinger, O.W. & Shyprykevic, P. (1998). Analysis of composite laminates with multiple fasteners", *Int. J. of Solids & Structures*, vol. 35, pp. 1793-1811, ISSN 0020-7683;

Moon, Y.H.; Kang, S.S.; Cho, J.R. & Kim, T.G. (2003). Effect of tool temperature on the reduction of the springback of aluminum sheets, *J. Mater. Process. Technol.*, Vol 132 p. 365. doi:10.1016/S0924-0136(02)00925-1, ISSN 0924-0136;

Ryan, L.; Monaghan, J. (2000). Failure Mechanism of Riveted Joint in Fibre Metal Laminates, *J. of Materials Processing Technology*, vol. 103, pp. 36-43, ISSN 0924-0136;

Schiehlen, W. (2006). Computational dynamics: theory and applications of multibody systems, *European Journal of Mechanics A/Solids,* vol. 25, pp. 566–594, ISSN 0997-7538;

Schiehlen, W.; Guse, N. & Seifried, R. (2006). Multibody dynamics in computational mechanics and engineering applications, *Comput. Methods Appl. Mech. Engrg*, vol. 195, pp. 5509-5522, ISSN 0045-7825;

Severson, K.; Perlman, A.B. & Stringfellow, R. (2008). Quasi-static and dynamic sled testing of prototype commuter rail passenger seats, *Proceedings of the 2008 IEEE/ASME Joint Rail Conference, JRC2008*, ISBN 0791848124, April 22-23, 2008 Wilmington, Delaware, USA.

Urban, M.U. (2003). Analysis of the Fatigue Life of Riveted Sheet Metal Helicopter Airframe Joints, *Int. J. of Fatigue*, vol. 25, pp. 1013-1026, ISSN 0142-1123;

Zhang, J.; Park, J.H. & Atluri, S.N. (1997). Analytical Fatigue Life Estimation of Full-Scale Fuselage Panel, in: *Proc. of FAA-NASA Symposium on the Continute Airworthiness of Aircraft Structures, DOT/FAA/AR-97/2,* vol. 1, pp. 51-62, ISBN 87404-279-8, Atlanta, GA, August 28-29.

Numerical Simulations - Applications, Examples and Theory
Edited by Prof. Lutz Angermann

ISBN 978-953-307-440-5
Hard cover, 520 pages
Publisher InTech
Published online 30, January, 2011
Published in print edition January, 2011

This book will interest researchers, scientists, engineers and graduate students in many disciplines, who make use of mathematical modeling and computer simulation. Although it represents only a small sample of the research activity on numerical simulations, the book will certainly serve as a valuable tool for researchers interested in getting involved in this multidisciplinary ï¬eld. It will be useful to encourage further experimental and theoretical researches in the above mentioned areas of numerical simulation.

How to reference
In order to correctly reference this scholarly work, feel free to copy and paste the following:

Francesco Caputo and Alessandro Soprano (2011). Simulating the Response of Structures to Impulse Loadings, Numerical Simulations - Applications, Examples and Theory, Prof. Lutz Angermann (Ed.), ISBN: 978-953-307-440-5, InTech, Available from: http://www.intechopen.com/books/numerical-simulations-applications-examples-and-theory/simulating-the-response-of-structures-to-impulse-loadings

INTECH
open science | open minds

InTech Europe
University Campus STeP Ri
Slavka Krautzeka 83/A
51000 Rijeka, Croatia
Phone: +385 (51) 770 447
Fax: +385 (51) 686 166
www.intechopen.com

InTech China
Unit 405, Office Block, Hotel Equatorial Shanghai
No.65, Yan An Road (West), Shanghai, 200040, China
中国上海市延安西路65号上海国际贵都大饭店办公楼405单元
Phone: +86-21-62489820
Fax: +86-21-62489821